Article

Not peer-reviewed version

FN9-10ELP, an ECM-Mimetic Fusion Protein, Suppresses Etoposide-Induced Senescence in Human Mesenchymal Stem Cells

Jun-hyeog Jang * and Su-Hyeon Jang

Posted Date: 31 July 2025

doi: 10.20944/preprints202507.2636.v1

Keywords: cellular senescence; hTMSCs; FN9-10ELP; ECM-mimetic biomaterial; etoposide; SASP; fibronectin; elastin-like polypeptide

 doi:10.20944/preprints202507.2636.v1

Article

FN9-10ELP, an ECM-Mimetic Fusion Protein, Suppresses Etoposide-Induced Senescence in Human Mesenchymal Stem Cells

Su-Hyeon Jang and Jun-Hyeog Jang *

Department of Biochemistry, Inha University School of Medicine, Incheon 22212, Korea

* Correspondence: juhjang@inha.ac.kr

Abstract

Background: Cellular senescence impairs the therapeutic potential of mesenchymal stem cells (MSCs), limiting their clinical applications. In this study, we aimed to evaluate whether fusion protein of fibronectin type III domains 9-10 and elastin-like polypeptide (FN9-10ELP), a recombinant extracellular matrix (ECM)-mimetic fusion protein composed of fibronectin type III domains 9 and 10 conjugated to elastin-like polypeptides, could suppress senescence induced by the chemotherapeutic agent etoposide in Human turbinate-derived mesenchymal stem cells (hTMSCs). **Methods:** Senescence was induced in hTMSCs by treatment with 20μM etoposide. The anti-senescence effects of FN9-10ELP were evaluated by assessing cell viability (MTT assay), senescence-associated gene expression (qRT-PCR), nuclear morphology (DAPI staining), and SA-β-galactosidase activity. **Results:** FN9-10ELP treatment significantly enhanced cell viability and attenuated the messenger ribonucleic acid (mRNA) expression of senescence-associated secretory phenotype (SASP) genes, including Interleukin-6 (IL-6), Interleukin-8 (IL8), and plasminogen activator inhibitor-1 (PAI-1). Furthermore, FN9-10ELP reduced etoposide-induced nuclear enlargement and decreased the proportion of SA-β-gal-positive cells, indicating attenuation of the senescence phenotype. **Conclusions:** FN9-10ELP suppresses etoposide-induced senescence in hTMSCs by preserving cell viability and reducing the expression of SASP factors and morphological senescence markers. These findings highlight the potential of ECM-mimetic proteins such as FN9-10ELP as promising biomaterials in regenerative medicine and anti-aging therapies.

Keywords: cellular senescence; hTMSCs; FN9-10ELP; ECM-mimetic biomaterial; etoposide; SASP; fibronectin; elastin-like polypeptide

1. Introduction

Human mesenchymal stem cells (hMSCs) are highly susceptible to senescence during in vitro expansion or upon exposure to genotoxic stress, which significantly compromises their regenerative capacity and limits their clinical utility in cell-based therapies [1,2]. Senescent hMSCs exhibit hallmark features such as enlarged morphology, elevated senescence-associated β-galactosidase (SA-β-gal) activity, and increased expression of pro-inflammatory cytokines and matrix-degrading enzymes, collectively known as the SASP [3,4]. Therefore, developing strategies to delay or suppress senescence in hMSCs is essential for improving the efficacy of regenerative stem cell therapies.

ECM-mimetic biomaterials have garnered increasing attention for their ability to replicate native cellular environments and modulate stem cell behavior [4]. FN9-10ELP, the core material used in this study, is a recombinant ECM-based fusion protein designed to regulate cellular functions such as adhesion, proliferation, and survival. Emerging evidence indicates that the ECM is not merely a structural scaffold, but actively influences cellular behavior—including senescence—through integrin-mediated signaling pathways, affecting processes such as deoxyribonucleic acid (DNA) repair, oxidative stress response, and inflammation [5,6]. Notably, alterations in ECM composition or

 doi:10.20944/preprints202507.2636.v1

stiffness can exacerbate senescence by modulating focal adhesion kinase (FAK), mitogen-activated protein kinase (MAPK), and phosphatidylinositol 4,5-bisphosphate 3-kinase/AKT (PI3K/AKT) signaling pathways [7,8], whereas restoration of ECM-like conditions has been shown to reduce senescence markers and promote cellular rejuvenation [9].

Fibronectin (FN), a key ECM component, contains functional domains (type III repeats 9 and 10; FN9-10) that harbor an RGD motif and synergy site (PHSRN), which are essential for binding integrins such as $\alpha5\beta1$ and $\alpha v\beta3$, triggering downstream signaling [10–12]. Elastin-like polypeptides (ELPs) are artificial, thermoresponsive biopolymers composed of VPGXG repeats (where X is any amino acid except proline) that exhibit reversible phase transition behavior [13,14]. ELPs are highly biocompatible, biodegradable, and exhibit low immunogenicity, making them attractive platforms for biomedical applications including drug delivery, tissue engineering, and surface modification [13–15]. Moreover, ELPs can be genetically fused to functional domains like FN9-10 to produce ECM-mimetic biomaterials with enhanced protein stability and biological activity.

Mesenchymal stem cells (MSCs), a type of adult stem cell with multipotent differentiation potential, have attracted significant attention for their therapeutic potential in tissue repair and immunomodulation [16]. hTMSCs used in this study have recently been recognized as a highly promising cell source among various tissue-derived MSCs due to their ease of harvest, high viability and proliferation, and multipotent differentiation capacity, making them suitable for clinical applications [17]. Indeed, turbinate-derived cells have been reported to possess differentiation potential into osteogenic, chondrogenic, and adipogenic lineages [17,18]. Moreover, they have demonstrated immunomodulatory capabilities by regulating the secretion of various cytokines, including IL-6, IL-8, and Tumor Necrosis Factor-Alpha (TNF-α), in response to inflammatory stimuli such as Toll-like receptors (TLRs) [19]. However, like other MSCs, hTMSCs are susceptible to cellular senescence during prolonged in vitro culture or under external stress conditions, leading to diminished stem cell properties and functions, which may limit their clinical applicability [20]. Specifically, premature senescence induced by DNA damage is a common response under external stress conditions [21], and the etoposide-induced senescence model, using the topoisomerase II inhibitor etoposide, is widely employed to experimentally replicate this process [22,23]. Etoposide, a well-known chemotherapeutic agent, induces DNA double-strand breaks (DSBs) during DNA replication and transcription by inhibiting topoisomerase II activity, which leads to sustained activation of the DNA damage response (DDR) and subsequently causes cellular senescence and apoptosis [24,25], and in this study, it was used to establish a cellular senescence model.

Previous studies have demonstrated that the FN9-10ELP fusion protein improves MSCs adhesion and proliferation, potentially contributing to the maintenance of stem cell functions [26,27]. However, it remains unclear whether FN9-10ELP can attenuate cellular senescence in hTMSCs under DNA damage-induced stress.

Accordingly, this study analyzed the effects of FN9-10ELP coating, an ECM-based biomaterial, on etoposide-induced cellular senescence in hTMSCs. The anti-senescent effect of FN9-10ELP was evaluated in an etoposide-induced senescence model by assessing cell viability, expression of senescence-associated genes, nuclear morphology, and SA-β-gal activity. This study suggests that FN9-10ELP may be effective in maintaining the viability of hTMSCs and attenuating senescence under senescence-inducing conditions, and that it could contribute to the development of stem cell-based strategies for regenerative medicine and anti-aging therapies.

2. Materials and Methods

2.1. Construction and Expression of Recombinant FN9-10ELP Fusion Protein

As previously described [26], an ELP coding sequence was designed using Val, Leu, and Gly at a 17:4:9 ratio as guest residues. The full ELP[V17L4G9-30] sequence, synthesized by Genotech (Daejeon, Korea), incorporated these residues at the fourth position (Xaa) of the pentapeptide repeat (Val-Pro-Gly-Xaa-Gly). The sequence was amplified by PCR and cloned into the pBAD-His-FNIII9-

 doi:10.20944/preprints202507.2636.v1

10 vector using *Sac*I and *Hind*III restriction sites. The resulting construct was transformed into *E. coli* TOP10 for recombinant protein expression. For expression, transformed *E. coli* were cultured overnight at 37 °C in Luria Broth containing ampicillin (LB-Amp). When cultures reached an OD_{600} of 0.6, protein expression was induced by the addition of 0.1% (w/v) L-arabinose. After 6 hours of induction, cells were harvested by centrifugation at 6,000 × g for 10 miniutes, lysed, and sonicated. The soluble fraction was collected by centrifugation at 13,000 × g for 25 minutes at 4 °C. Crude FN9-10ELP fusion protein was isolated by adding 3 M NaCL to the supernatant, incubating at 40 °C, and centrifuging at the same temperature. The resulting pellet was resuspended in ice-cold 1× phosphate-buffered saline (PBS), followed by a final centrifugation at 4 °C to increase purity. Protein purity was confirmed by 12% SDS-PAGE and Coomassie Brilliant Blue staining.

2.2. hTMSCs Culture and Preparation

hMSCs were derived from nasal inferior turbinate tissues obtained from patients prior to surgery. This study was approved by the Institutional Review Board (IRB) of the Catholic University Seoul St. Mary's Hospital (approval number KC08TISS0341). Detailed methods for isolation and culture of hMSCs were have been previously reported [28].

hTMSCs were cultured in α-minimal essential medium (α-MEM; Welgene, Gyeongsan, Korea) supplemented with 10% fetal bovine serum (FBS; Welgene, Gyeongsan, Korea), 100μg/mL streptomycin, and 100 U/mL penicillin G sodium, in a 37 °C incubator with 5% CO_2. When the cells reached approximately 70% confluence, they were detached using 0.25% trypsin-EDTA and passaged into new culture dishes with a diameter of 100mm. Cells used for senescence attenuation experiments were prepared by replacing the culture medium with 1% FBS-containing medium one day prior to the experiments.

2.3. Cell proliferation Assay

The proliferative effect of FN9-10ELP on cells was evaluated using the MTT assay [3-(4,5-dimethylthiazol-2-yl)-2,5-diphenyltetrazolium bromide; AMRESCO Inc., Solon, USA]. The MTT assay is a quantitative method that indirectly reflects cell viability and proliferation based on cellular metabolic activity. FN9-10ELP was coated onto a 4-well plate at a concentration of 1 μg/cm^2, followed by overnight incubation at 4 °C. hTMSCs were seeded onto both the FN9-10ELP-coated plates and non-coated plates(control) at a density of 3 × 10^4 cells/well and incubated for 1-2 hours at 37 °C in a 5% CO_2 incubator to allow for cell attachment. Subsequently, cellular senescence was induced by treating the cells with 20 μM etoposide, and cells were cultured for 0, 1, and 2 days. At each time point, cells were washed with Dulbecco's phosphate-buffered saline (DPBS), followed by the addition of 50 μL of 5 mg/mL MTT solution to each well. The plates were incubated for 1 hour at 37 °C in a 5% CO_2 incubator. After incubation, the MTT solution was removed, and 100 μL of dimethyl sulfoxide (DMSO) was added to each well to dissolve the formazan crystals for 30 minutes. Cell viability was quantified by measuring absorbance at 540 nm using a micropalte reader.

2.4. RNA Extraction and cDNA Synthesis

hTMSCs were cultured for 2 days on 100mm culture dishes non-coated (control) and coated with FN9-10ELP at a concentration of 1 μg/cm^2. Total RNA was extracted using the Easy-spin™ Total RNA Extraction Kit (iNtRON Biotechnology, Seoul, Republic of Korea) according to the manufacturer's instructions. The purity and concentration of the extracted RNA were assessed by measuring absorbance at 260nm and 280 nm using a NanoDrop 2000 spectrophotometer (Thermo Scientific, Waltham, MA, USA). Only RNA samples with an A260/A280 ratio between 1.9 and 2.1 were selected for subsequent analysis.

For reverse transcription, 2 μg of total RNA was used in a 20 μL reaction mixture. The reaction mixture contained 2 μL of 10× RT random primer (Invitrogen, USA), 0.6 μL of 25× dNTP mix (Bioline, UK), 2 μL of enzyme buffer (Applied Biosystems, USA), and 1 μL of M-MLV Reverse Transcriptase

 doi:10.20944/preprints202507.2636.v1

(Invitrogen, USA). The reverse transcription reaction was carried out at 37 °C for 2 hours, followed by enzyme inactivation at 85 °C for 5 minutes. The resulting complementary DNA (cDNA) was stored at -20 °C until further use.

2.5. Quantitative Real-Time PCR Analysis

The mRNA expression levels of senescence-related genes (IL-6, IL-8, PAI-1) and the internal control gene β-actin were analyzed by quantitative real-time polymerase chain reaction (qRT-PCR). The primer sequences for each gene are listed in Table 1. All qRT-PCR reactions were performed using the StepOne™ Real-Time PCR System (Applied Biosystems, Waltham, MA, USA).

Each PCR reaction was carried out in a total volume of 15 μL, containing template cDNA, gene-specific primers, and 2× qPCR SYBR Green Master Mix (Cat. No. T22O4V2, Applied Biosystems, Waltham, MA, USA).

The thermal cycling conditions were as follows: initial enzyme activation at 95 °C for 1 minute, followed by 45 cycles of denaturation at 95 °C for 15 seconds, annealing at 55 °C for 15 seconds, and extension at 72 °C for 45 seconds. The threshold cycle (Ct) values obtained after amplification were used for the quantitative analysis of gene expression.

Table 1. Sequence of primer used in the real-time PCR.

Genes	Forward primer	Reverse primer
β-actin	TGGCACCCAGCACAATGAAGAT	TACTCCTGCTTGCTGATCCA
IL-6	CCCCTGACCCAACCACAAAT	GCCCAGTGGACAGGTTTCTG
IL-8	GTCTGCTAGCCAGGATCCAC	AGTGCTTCCACATGTCCTCA
PAI-1	CAGACCAAGAGCCTCTCCAC	GGTTCCATCACTTGGCCCAT

2.6. DAPI Staining and Nuclear Size Analysis

FN9-10ELP was applied to 12-well plates at a concentration of 1 μg/cm² and coated overnight at 4 °C. hTMSCs were seeded onto FN9-10ELP-coated and non-coated control wells at a density of 2 × 10^5 cells per well and incubated at 37 °C in a 5% CO_2 incubator for 1-2 hours to allow cell attachment. Etoposide was then added at a final concentration of 20 μM to induce cellular senescence, and cells were cultured for 5 days.

Cultured cells were fixed with 3.7% formaldehyde for 10 minutes at 37 °C in a 5% CO_2 incubator and then washed with DPBS. Permeabilization was performed using 0.5% Triton X-100 for 15 minutes, followed by another wash with DPBS. The fixed and permeabilized cells were stained with 4′,6′-Diamidino-2-phenylindole (DAPI) solution for 15 minutes and subsequently washed three times with DPBS.

Fluorescent images were captured using a fluorescence microscope (Olympus IX83, Olympus Corp., Tokyo, Japan), and nuclear size was analyzed using Fiji software (based on ImageJ; NIH, Bethesda, MD, USA, https://imagej.net/software/fiji/downloads).

2.7. Senescence-Associated β-Galactosidase (SA-β-gal) Staining

SA-β-gal staining was performed using the Cell Senescence β-Galactosidase Staining Kit (MCE, HY-K1089, USA) according to the manufacturer's protocol to analyze SA-β-gal activity in cultured cells. FN9-10ELP was applied to 12-well plates at a concentration of 1 μg/cm² and coated overnight at 4 °C.

Subsequently, hTMSCs were seeded onto the FN9-10ELP-coated plates and non-coated control plates at a density of 5 × 10^4 cells/well, and incubated at 37 °C in a 5% CO_2 incubator for 1-2 hours to allow cell attachment. Cellular senescence was induced by treating the cells with 20 μM etoposide, and the cells were cultured for 5 days.

 doi:10.20944/preprints202507.2636.v1

SA-β-gal-positive cells were observed using a bright-field microscope at 20× magnification. The total number of cells was determined by DAPI staining, and the percentage of SA-β-gal positive cells was calculated using the following formula: (Number of positive cells / Total number of cells) × 100.

2.8. Statistical Analysis

All data are presented as mean ± standard error of the mean (SEM). Statistical significance between two groups was analyzed using Welch's t-test, and a p-value less than 0.05 was considered statistically significant. All statistical analyses were performed using R statistical software (R Project for Statistical Computing, version 4.4.3, https://www.r-project.org/). Statistical significance is indicated as follows: $p < 0.05$ (*), $p < 0.01$ (**), $p < 0.001$ (***), and $p < 0.0001$ (****).

3. Results

3.1. FN9-10ELP Protects hTMSCs from Etoposide-Induced Cellular Senescence by Promoting Viability

To evaluate whetehr the recombinant ECM-mimetic fusion protein FN9-10ELP can attenuates etoposide-induced senescence in hTMSCs, cell viability was assessed using the MTT assay (Figure 1). On day 0, there was no sighnificant difference in absorbance between the FN9-10ELP group and the control group, indicating similar initial cell attachment and viability. However, on day 1, the absorbance of the FN9-10ELP group was significantly higher than that of the control group ($p < 0.05$), and this effect became even more pronounced on day 2 ($p < 0.001$). These results demonstrate that FN9-10ELP effectively enhances the viability of hTMSCs in a time-dependent manner under etoposide-induced senescence conditions and indirectly suggest its role in attenuating cellular senescence. Notably, the anti-senescent effect of FN9-10ELP was evident as early as day 1 and was further enhanced by day 2.

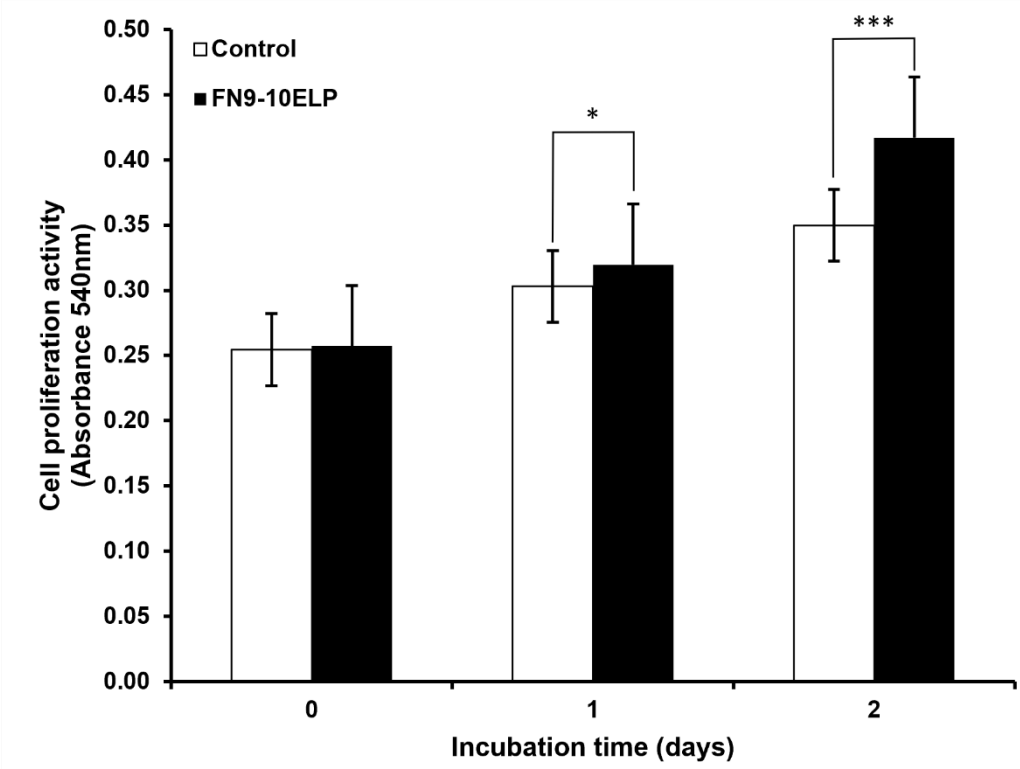

Figure 1. Analysis of hTMSCs viability under etoposide (20 μM) treatment in the presence or absence of FN9-10ELP. hTMSCs were cultured under two conditions: with FN9-10ELP coating (1 μg/cm²) and non-coating (control). Cellular senescence was induced by treating both groups with etoposide (20 μM). MTT assays were performed on days 0, 1, and 2, and absorbance measurements were used as an indicator of cell viability. The FN9-10ELP group showed significantly higher viability than the control group from day 1, and the difference

 doi:10.20944/preprints202507.2636.v1

became more pronounced on day 2. Data are presented as mean ± SEM, and statistical significance was determined using an unpaired, two-tailed Welch's t-test (*$p < 0.05$, ***$p < 0.001$).

3.2. FN9-10ELP Suppresses the Expression of Senescence-Associated Genes in Etoposide-Treated hTMSCs

To evaluate the anti-senescent effect of FN9-10ELP, hTMSCs were cultured on 100 mm dishes coated with FN9-10ELP and non-coated (control), followed by treatment with 20 μM etoposide for two days to induce cellular senescence. The mRNA expression levels of the senescence-associated genes IL-6, IL-8, and PAI-1 were measured using real-time PCR, with β-actin used as an internal control. As a result, the expression of all three genes was significantly decreased in the FN9-10ELP condition. Both IL-6 and IL-8 were significantly downregulated following FN9-10ELP treatment ($p < 0.05$), and PAI-1 expression showed a more significant reduction ($p < 0.01$) (Figure 2). These results suggest that FN9-10ELP effectively suppresses the expression of senescence-associated genes under etoposide-induced stress conditions, supporting its potential role in modulating cellular senescence in hTMSCs.

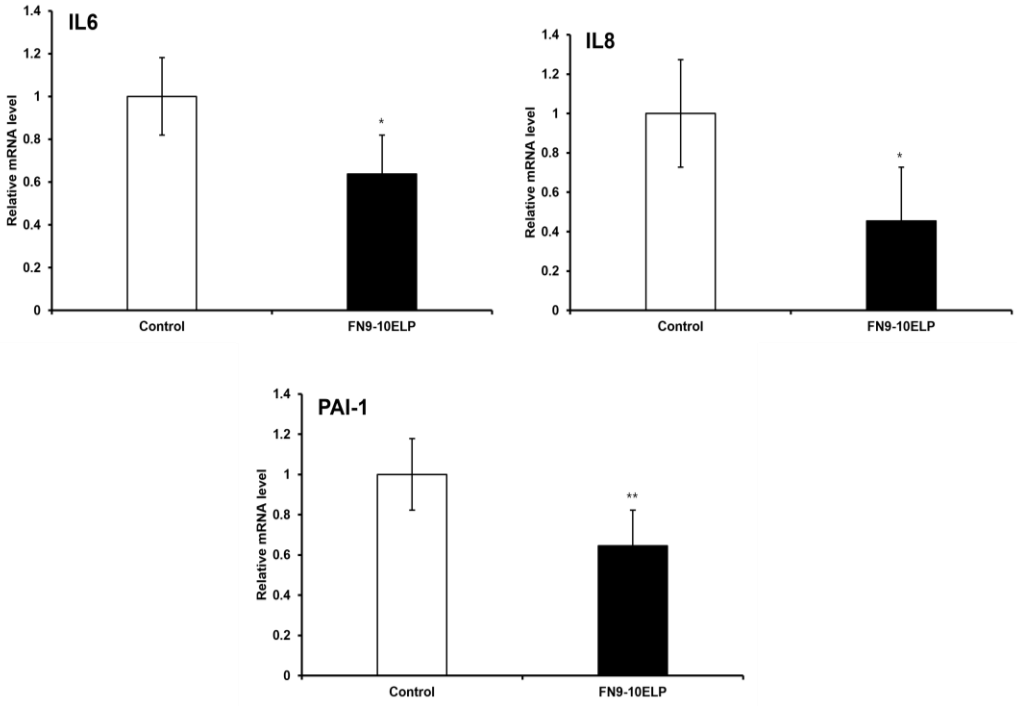

Figure 2. FN9-10ELP suppresses the expression of senescence-associated genes in etoposide-treated hTMSCs. To induce senescence, hTMSCs were treated with 20 μM etoposide for two days and cultured on FN9-10ELP dishes and control dishes. The mRNA levels of IL-6, IL-8, and PAI-1 were analyzed by real-time PCR, and the expression levels were normalized to β-actin and presented as relative expression. All three genes were significantly downregulated in the FN9-10ELP group, indicating that FN9-10ELP attenuates the transcriptional activation of senescence-associated genes. Data are presented as mean ± SEM, and statistical significance was determined using an unpaired, two-tailed Welch's t-test (*$p < 0.05$, **$p < 0.01$).

3.3. FN9-10ELP Attenuates Nuclear Enlargement Induced by Etoposide

To evaluate whether FN9-10ELP can attenuate etoposide-induced cellular senescence, we examined nuclear morphology via DAPI staining. As shown in Figure 3, the nuclear area significantly increased in the control group (4338.45 μm²). In contrast, cells cultured on FN9-10ELP-coated surfaces exhibited a significantly reduced nuclear area (3438.61 μm²). Statistical analysis revealed a highly significant difference between the two groups ($p < 0.001$), suggesting that FN9-10ELP effectively attenuates nuclear enlargement associated with cellular senescence. These findings indicate that FN9-

 doi:10.20944/preprints202507.2636.v1

10ELP may serve as a functional biomaterial capable of partially alleviating etoposide-induced cellular senescence in hTMSCs by attenuating nuclear hypertrophy.

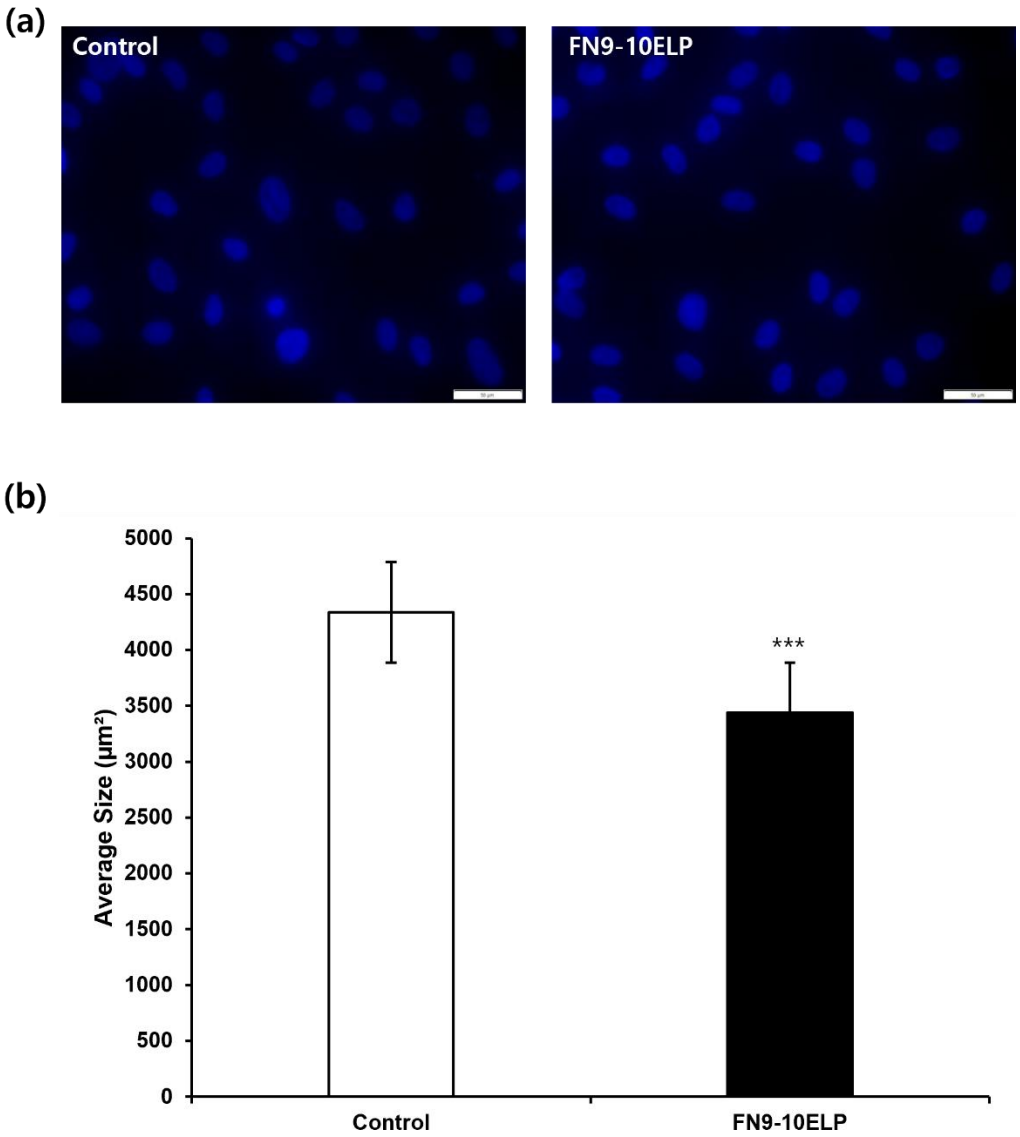

Figure 3. FN9-10ELP attenuates etoposide-induced nuclear enlargement in hTMSCs. (a) Representative fluorescence images of DAPI-stained hTMSCs treated with etoposide under control and FN9-10ELP treatment conditions (Scale bar = 50 μm). (b) Quantification of nuclear size (μm²) graph. After treatment with 20μM etoposide for 5 days, nuclear area was quantitatively analyzed. Nuclear area was significantly increased in the control group (4338.45 μm²), while it was significantly decreased in the FN9-10ELP group (3438.61 μm²). Data are presented as mean ± SEM, and statistical significance was determined using an unpaired, two-tailed Welch's t-test (***$p < 0.001$).

3.4. FN9-10ELP Significantly Suppresses Etoposide-Induced SA-β-Galactosidase Activitity in Senescent hTMSCs

To evaluate the anti-senescence effect of FN9-10ELP in hTMSCs under an etoposide-induced cellular senescence model, SA-β-gal staining was performed. As shown in Figure 4, the proportion of SA-β-gal-positive cells in the control group was 66.44%, whereas it significantly decreased to 37.24% in the FN9-10ELP group ($p < 0.001$). These results suggest that FN9-10ELP effectively suppresses etoposide-induced cellular senescence in hTMSCs.

 doi:10.20944/preprints202507.2636.v1

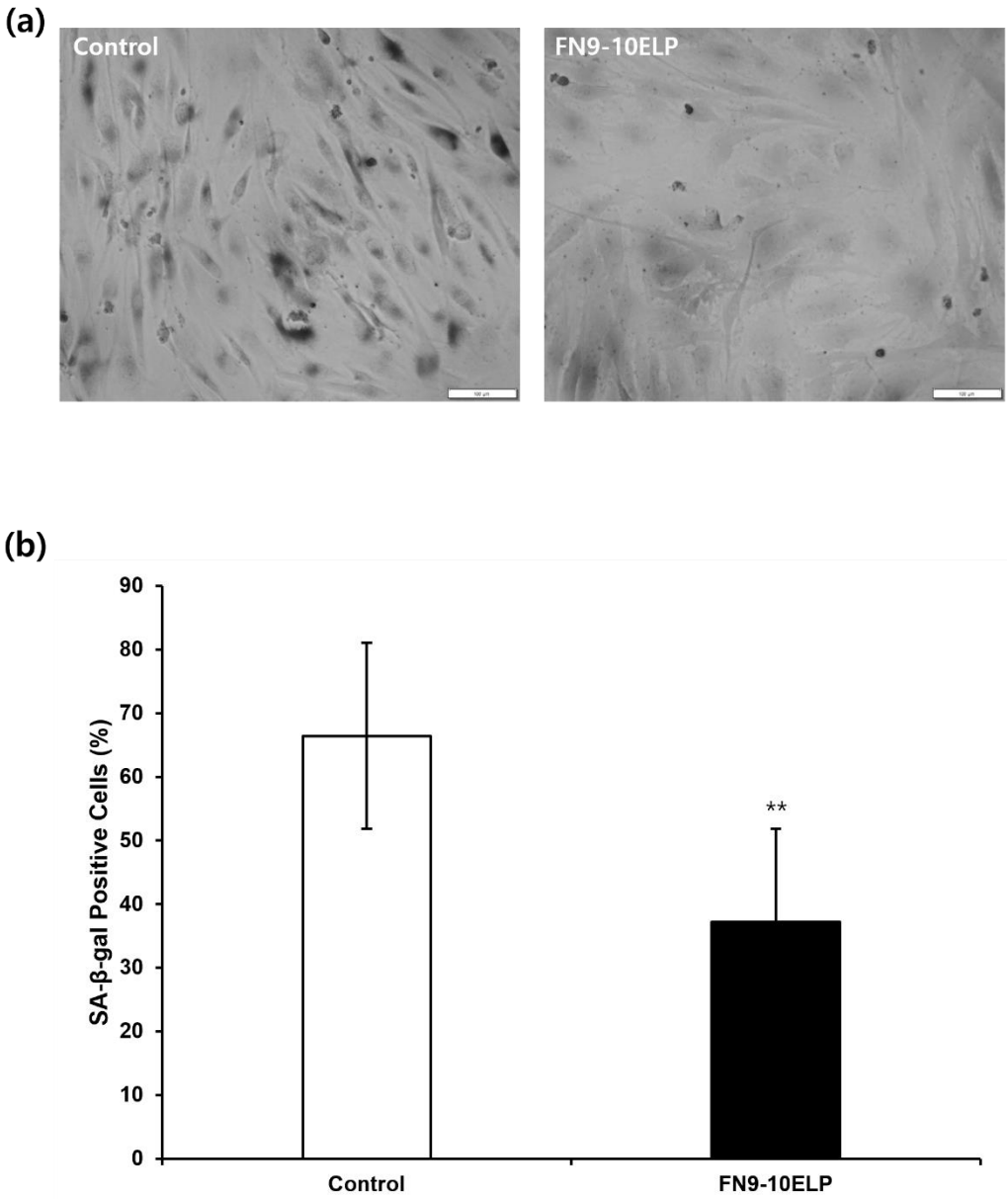

Figure 4. FN9-10ELP attenuates etoposide-induced cellular senescence in hTMSCs. (a) Representative images of SA-β-gal stained hTMSCs treated with etoposide under control and FN9-10ELP treatment conditions (Scale bar = 100 μm). (b) Quanti-fication graph of SA-β-gal-positive cells as a percentage of total cells. Cellular senescence in hTMSCs was evaluted by SA-β-gal stainig after treatment with 20 μM etoposide for 5 days. Cells were seeded at a density of 5×10^4 cells/well in a 12-well plate. The proportion of SA-β-gal positive cells was significantly lower in the FN9-10ELP group compared to the control group. Data are presented as mean ± SEM, and statistical significance was determined using an unpaired, two-tailed Welch's t-test (**$p < 0.01$).

4. Discussion

Although cellular senescence has been extensively investigated in the context of aging, tissue dysfunction, and stem cell exhaustion, its impact on mesenchymal stem cells (MSCs)—which play a critical role in tissue regeneration and repair—has not been fully elucidated. In this study, we demonstrated that the recombinant ECM-mimetic fusion protein FN9-10ELP effectively suppresses etoposide-induced senescence in hTMSCs. Under FN9-10ELP condition, cell viability was enhanced, the expression of SASP factors such as IL-6, IL-8, and PAI-1 was reduced, and morphological senescence indicators including nuclear size and SA-β-gal activity were significantly decreased.

 doi:10.20944/preprints202507.2636.v1

These results suggest that FN9-10ELP serves as a key modulator of cellular senescence, contributing to the preservation of the regenerative capacity of human mesenchymal stem cells.

To assess whether FN9-10ELP, a recombinant ECM-mimetic fusion protein, could suppress cellular senescence in hTMSCs induced by etoposide (20 μM), cell viability was evaluated using the MTT assay (Figure 1). On day 0, no significant difference in absorbance was observed between the FN9-10ELP-coated group and the non-coated group, indicating similar levels of initial cell attachment and viability. However, by day 1, the FN9-10ELP group showed significantly higher absorbance values compared to the control ($p < 0.05$), and this difference became even more pronounced on day 2 ($p < 0.001$). These findings suggest that FN9-10ELP enhances the viability of hTMSCs under DNA damage-induced senescent conditions in a time-dependent manner, possibly by preserving cellular metabolic activity and increasing resistance to apoptosis or senescence. Notably, the significant difference observed on day 2 indicates an accumulative anti-senescent effect of FN9-10ELP over time. Lee et al. (2019) reported that FN9-10ELP-coated plates promote adhesion and proliferation of MSCs [26], and Park et al. (2021) demonstrated that FN9-10ELP coating on titanium surfaces significantly enhanced hMSCs attachment and proliferation [27]. These studies support our findings that FN9-10ELP protects hTMSCs from etoposide-induced stress and promotes cell survival. Given that mesenchymal stem cells (MSCs) are pivotal in tissue regeneration and anti-aging research, the observed enhancement of their viability by FN9-10ELP underscores its therapeutic potential.

qRT-PCR analysis revealed that the expression of senescence-associated genes—IL-6, IL-8, and PAI-1—was significantly reduced in FN9-10ELP-coated hTMSCs compared to non-coated controls (Figure 2). PAI-1 is a key factor known to amplify cellular senescence by enhancing the production of SASP components such as IL-6 and IL-8 [29], while IL-6 and IL-8 are representative SASP markers that are induced by DNA damage and contribute to proinflammatory microenvironments [30,31]. The downregulation of these genes suggests that FN9-10ELP may attenuate senescence by attenuating inflammatory signaling pathways.

Quantitative analysis of nuclear size via DAPI staining further supported the anti-senescent effects of FN9-10ELP. hTMSCs cultured on FN9-10ELP-coated surfaces displayed significantly smaller nuclear areas than those on non-coated surfaces (Figure 3). Nuclear and cellular enlargement is a well-established morphological hallmark of senescent cells. Indeed, Pathak et al. (2021) reported abnormal nuclear morphology and enlargement in senescent cells [32], and Heckenbach et al. (2022) quantitatively demonstrated increased nuclear size in both replicative and ionizing radiation-induced senescence models [33]. Therefore, the reduced nuclear area observed in FN9-10ELP-coated conditions suggests a delay or attenuation of senescence-associated morphological alterations.

Consistent with this, SA-β-gal staining revealed that the proportion of SA-β-gal-positive cells was significantly lower in the FN9-10ELP-coated group compared to the control (Figure 4). SA-β-galactosidase is a well-established biomarker of cellular senescence [34], and the reduced enzymatic activity observed here supports the anti-senescent effect of FN9-10ELP. Similarly, Tragoonlugkana et al. (2024) reported that adipose-derived stem cells (ADSCs) cultured on fibronectin (FN) or vitronectin (VN)-coated surfaces exhibited significantly fewer SA-β-gal-positive cells compared to non-coated controls [35]. Although different cell types were used, these findings are in agreement with our results and support the notion that ECM protein coatings can attenuates stem cells senescence. Hence, FN9-10ELP, an ECM-mimetic protein, demonstrates potential as a functional biomaterial for senescence attenuation.

Our findings suggest that FN9-10ELP not only serves as a mechanical support for cell attachment, but also modulates intracellular signaling to suppress cellular senescence. The FNⅢ9-10 domain is known to interact with integrin $\alpha 5\beta 1$ or $\alpha v\beta 3$ through its RGD motif, thereby activating signaling pathways such as FAK, P13K/AKT, and MAPK/p38, which are involved in promoting cell survival, regulating inflammation, and delaying senescence [36,37]. FN9-10ELP likely exerts its effects through modulation of these pathways, contributing to SASP attenuation and suppression of senescence-related morphological changes.

 doi:10.20944/preprints202507.2636.v1

Moreovers, the ELP domain enhances protein stability and surface adsorption, thereby improving the biological activity of the FN9-10 domain. For instance, FN9-10ELP fusion proteins have been shown to promote hMSCs adhesion and proliferation [26], and ELP derivatives containing RGD or YIGSR ligands have been reported to enhance fibroblast adhesion and growth [15]. These findings suggest that ELP improves cell-ECM interactions, thereby enhancing stem cell function and delaying senescence.

Despite the promising findings, this study has limitations. Further research is needed to clarify the molecular mechanisms of FN9-10ELP, including its effects on integrin and downstream signaling pathways. Additionally, the long-term impact of FN9-10ELP on stemness and differentiation potential remains to be investigated.

Nevertheless, this study demonstrates that FN9-10ELP can effectively suppress hTMSCs senescence and promote cell viability. FN9-10ELP has previously been reported to enhance hMSCs attachment and proliferation when coated on titanium surfaces [27], supporting its potential utility in tissue engineering applications. Future studies should investigate its applicability on various biomaterial surfaces, such as hydrogels and polymer scaffolds. These findings collectively highlight FN9-10ELP as a promising ECM-mimetic biomaterial for stem cell-based tissue regeneration and anti-aging therapeutics.

5. Conclusions

This study demonstrates that FN9-10ELP, a recombinant ECM-mimetic fusion protein, effectively suppresses etoposide-induced cellular senescence in hTMSCs. FN9-10ELP not only improves cell viability but also downregulates key senescence-associated genes (IL-6, IL-8, PAI-1), reduces nuclear enlargement, and significantly lowers SA-β-gal activity. These effects suggest that FN9-10ELP suppresses senescence by modulating the cellular microenvironment and potentially influencing integrin-mediated signaling pathways such as FAK/AKT/MAPK. Given its structural stability and biofunctionality, FN9-10ELP holds considerable promise as a functional biomaterial for enhancing stem cell viability and delaying senescence. Future studies should investigate its molecular mechanisms in detail and evaluate its efficacy in long-term cultures and in vivo regenerative models to further validate its clinical applicability.

Supplementary Materials: The following supporting information can be downloaded at the website of this paper posted on Preprints.org.

Author Contributions: Conceptualization, S.H.J. and J.H.J.; methodology, S.H.J.; validation, S.H.J. and J.H.J.; formal analysis, S.H.J.; investigation, S.H.J.; resources, J.H.J.; data curation, S.H.J.; writing—original draft preparation, S.H.J.; writing—review and editing, J.H.J.; supervision, J.H.J. All authors have read and agreed to the published version of the manuscript.

Funding: This work was supported by the National Research Foundation of Korea (NRF) grants funded by the Korean government (MSIT) (RS-2023-00208339) and INHA UNIVERSITY Research Grant.

Institutional Review Board Statement: The study was conducted in accordance with the Declaration of Helsinki and approved by the Institutional Review Board of the Catholic University of Korea, Seoul St. Mary's Hospital (protocol code KC08TISS0341).

Informed Consent Statement: Informed consent was obtained from all subjects involved in the study.

Data Availability Statement: Data supporting the findings of this study are available upon request from the corresponding author.

Conflicts of Interest: The authors declare no conflicts of interest.

 doi:10.20944/preprints202507.2636.v1

Abbreviations

The following abbreviations are used in this manuscript:

DAPI	4′,6′-Diamidino-2-phenylindole
DDR	DNA damage response
DMSO	Dimethyl Sulfoxide
DNA	Deoxyribonucleic Acid
DPBS	Dulbecco's Phosphate-Buffered Saline
DSBs	DNA double-strand breaks
ECM	Extracellular Matrix
ELPs	Elastin-like polypeptides
FAK	Focal Adhesion Kinase
FN	Fibronectin
FN9-10ELP	fusion protein of fibronectin type III domains 9-10 and elastin-like polypeptide
hMSCs	Human mesenchymal stem cells
hTMSCs	Human turbinate-derived mesenchymal stem cells
IL-6	Interleukin-6
IL-8	Interleukin-8
LB-Amp	Luria Broth containing ampicillin
MAPK	Mitogen-Activated Protein Kinase
mRNA	Messenger Ribonucleic Acid
MTT	3-(4,5-dimethylthiazol-2-yl)-2,5-diphenyltetrazolium bromide
PAI-1	Plasminogen Activator Inhibitor-1
PI3K	phosphatidylinositol 4,5-bisphosphate 3-kinase
qRT-PCR	Quantitative Real-Time Polymerase Chain Reaction
SA- β-gal	Senescence-Associated β-Galactosidase
SASP	Senescence-Associated Secretory Phenotype
SDS-PAGE	Sodium Dodecyl Sulfate-Polyacrylamide Gel Electrophoresis
SEM	Standard Error of the Mean
TLRs	Toll-like receptors
TNF- α	Tumor Necrosis Factor-Alpha
α-MEM	α-minimal essential medium

References

1. Campisi, J. "Aging, Cellular Senescence, and Cancer." *Annu Rev Physiol* 75 (2013): 685–705.
2. Lopez-Otin, C., M. A. Blasco, L. Partridge, M. Serrano, and G. Kroemer. "The Hallmarks of Aging." *Cell* 153, no. 6 (2013): 1194–217.
3. Childs, B. G., M. Gluscevic, D. J. Baker, R. M. Laberge, D. Marquess, J. Dananberg, and J. M. van Deursen. "Senescent Cells: An Emerging Target for Diseases of Ageing." *Nat Rev Drug Discov* 16, no. 10 (2017): 718–35.
4. Munoz-Espin, D., and M. Serrano. "Cellular Senescence: From Physiology to Pathology." *Nat Rev Mol Cell Biol* 15, no. 7 (2014): 482–96.
5. Blokland, K. E. C., S. D. Pouwels, M. Schuliga, D. A. Knight, and J. K. Burgess. "Regulation of Cellular Senescence by Extracellular Matrix during Chronic Fibrotic Diseases." *Clin Sci (Lond)* 134, no. 20 (2020): 2681–706.
6. Jean, C., P. Gravelle, J. J. Fournie, and G. Laurent. "Influence of Stress on Extracellular Matrix and Integrin Biology." *Oncogene* 30, no. 24 (2011): 2697–706.
7. El-Rashidy, A. A., S. El Moshy, I. A. Radwan, D. Rady, M. M. S. Abbass, C. E. Dorfer, and K. M. Fawzy El-Sayed. "Effect of Polymeric Matrix Stiffness on Osteogenic Differentiation of Mesenchymal Stem/Progenitor Cells: Concise Review." *Polymers (Basel)* 13, no. 17 (2021).
8. Wang, C., X. Jiang, B. Huang, W. Zhou, X. Cui, C. Zheng, F. Liu, J. Bi, Y. Zhang, H. Luo, L. Yuan, J. Yang, and Y. Yu. "Inhibition of Matrix Stiffness Relating Integrin Beta1 Signaling Pathway Inhibits Tumor Growth in Vitro and in Hepatocellular Cancer Xenografts." *BMC Cancer* 21, no. 1 (2021): 1276.

 doi:10.20944/preprints202507.2636.v1

9. Choi, H. R., K. A. Cho, H. T. Kang, J. B. Lee, M. Kaeberlein, Y. Suh, I. K. Chung, and S. C. Park. "Restoration of Senescent Human Diploid Fibroblasts by Modulation of the Extracellular Matrix." *Aging Cell* 10, no. 1 (2011): 148–57.
10. Kim, S. H., J. Turnbull, and S. Guimond. "Extracellular Matrix and Cell Signalling: The Dynamic Cooperation of Integrin, Proteoglycan and Growth Factor Receptor." *J Endocrinol* 209, no. 2 (2011): 139–51.
11. Altroff, H., R. Schlinkert, C. F. van der Walle, A. Bernini, I. D. Campbell, J. M. Werner, and H. J. Mardon. "Interdomain Tilt Angle Determines Integrin-Dependent Function of the Ninth and Tenth Fiii Domains of Human Fibronectin." *J Biol Chem* 279, no. 53 (2004): 55995–6003.
12. Aota, S., M. Nomizu, and K. M. Yamada. "The Short Amino Acid Sequence Pro-His-Ser-Arg-Asn in Human Fibronectin Enhances Cell-Adhesive Function." *Journal of Biological Chemistry* 269, no. 40 (1994): 24756–61.
13. Roberts, S., M. Dzuricky, and A. Chilkoti. "Elastin-Like Polypeptides as Models of Intrinsically Disordered Proteins." *FEBS Lett* 589, no. 19 Pt A (2015): 2477–86.
14. Despanie, J., J. P. Dhandhukia, S. F. Hamm-Alvarez, and J. A. MacKay. "Elastin-Like Polypeptides: Therapeutic Applications for an Emerging Class of Nanomedicines." *J Control Release* 240 (2016): 93–108.
15. Sarangthem, V., H. Sharma, R. Goel, S. Ghose, R. W. Park, S. Mohanty, T. K. Chaudhuri, A. K. Dinda, and T. D. Singh. "Application of Elastin-Like Polypeptide (Elp) Containing Extra-Cellular Matrix (Ecm) Binding Ligands in Regenerative Medicine." *Int J Biol Macromol* 207 (2022): 443–53.
16. Pittenger, M. F., A. M. Mackay, S. C. Beck, R. K. Jaiswal, R. Douglas, J. D. Mosca, M. A. Moorman, D. W. Simonetti, S. Craig, and D. R. Marshak. "Multilineage Potential of Adult Human Mesenchymal Stem Cells." *Science* 284, no. 5411 (1999): 143–47.
17. Kim, D. H., and S. H. Hwang. "Human Nasal Turbinate-Derived Stem Cells for Tissue Engineering and Regenerative Medicine." *J Rhinol* 31, no. 3 (2024): 133–37.
18. Kwon, J. S., S. W. Kim, D. Y. Kwon, S. H. Park, A. R. Son, J. H. Kim, and M. S. Kim. "In Vivo Osteogenic Differentiation of Human Turbinate Mesenchymal Stem Cells in an Injectable in Situ-Forming Hydrogel." *Biomaterials* 35, no. 20 (2014): 5337–46.
19. Hwang, S. H., H. K. Cho, S. H. Park, W. Lee, H. J. Lee, D. C. Lee, J. H. Oh, S. H. Park, T. G. Kim, H. J. Sohn, J. M. Kang, and S. W. Kim. "Toll Like Receptor 3 & 4 Responses of Human Turbinate Derived Mesenchymal Stem Cells: Stimulation by Double Stranded Rna and Lipopolysaccharide." *PLoS One* 9, no. 7 (2014): e101558.
20. Wagner, W., S. Bork, P. Horn, D. Krunic, T. Walenda, A. Diehlmann, V. Benes, J. Blake, F. X. Huber, V. Eckstein, P. Boukamp, and A. D. Ho. "Aging and Replicative Senescence Have Related Effects on Human Stem and Progenitor Cells." *PLoS One* 4, no. 6 (2009): e5846.
21. te Poele, R. H., A. L. Okorokov, L. Jardine, J. Cummings, and S. P. Joel. "DNA Damage Is Able to Induce Senescence in Tumor Cells in Vitro and in Vivo." *Cancer Res* 62, no. 6 (2002): 1876–83.
22. Malaise, O., Y. Tachikart, M. Constantinides, M. Mumme, R. Ferreira-Lopez, S. Noack, C. Krettek, D. Noël, J. Wang, C. Jorgensen, and J. M. Brondello. "Mesenchymal Stem Cell Senescence Alleviates Their Intrinsic and Seno-Suppressive Paracrine Properties Contributing to Osteoarthritis Development." *Aging (Albany NY)* 11, no. 20 (2019): 9128–46.
23. Huang, Y., S. Wang, D. Hu, L. Zhang, and S. Shi. "Alkbh5 Regulates Etoposide-Induced Cellular Senescence and Osteogenic Differentiation in Osteoporosis through Mediating the M(6)a Modification of Vdac3." *Sci Rep* 14, no. 1 (2024): 23461.
24. Tammaro, M., P. Barr, B. Ricci, and H. Yan. "Replication-Dependent and Transcription-Dependent Mechanisms of DNA Double-Strand Break Induction by the Topoisomerase 2-Targeting Drug Etoposide." *PLoS One* 8, no. 11 (2013): e79202.
25. Muslimovic, A., S. Nystrom, Y. Gao, and O. Hammarsten. "Numerical Analysis of Etoposide Induced DNA Breaks." *PLoS One* 4, no. 6 (2009): e5859.
26. Lee, S., J. E. Kim, H. J. Seo, and J. H. Jang. "Design of Fibronectin Type Iii Domains Fused to an Elastin-Like Polypeptide for the Osteogenic Differentiation of Human Mesenchymal Stem Cells." *Acta Biochim Biophys Sin (Shanghai)* 51, no. 8 (2019): 856–63.

 doi:10.20944/preprints202507.2636.v1

27. Park, B. H., E. S. Jeong, S. Lee, and J. H. Jang. "Bio-Functionalization and in-Vitro Evaluation of Titanium Surface with Recombinant Fibronectin and Elastin Fragment in Human Mesenchymal Stem Cell." *PLoS One* 16, no. 12 (2021): e0260760.
28. Hang Pham, L. B., Y. R. Yoo, S. H. Park, S. A. Back, S. W. Kim, I. Bjorge, J. Mano, and J. H. Jang. "Investigating the Effect of Fibulin-1 on the Differentiation of Human Nasal Inferior Turbinate-Derived Mesenchymal Stem Cells into Osteoblasts." *J Biomed Mater Res A* 105, no. 8 (2017): 2291–98.
29. Khoddam, Alireza, Douglas Vaughan, and Lisa Wilsbacher. "Role of Plasminogen Activator Inhibitor-1 (Pai-1) in Age-Related Cardiovascular Pathophysiology." *The Journal of Cardiovascular Aging* 5, no. 2 (2025).
30. Freund, A., A. V. Orjalo, P. Y. Desprez, and J. Campisi. "Inflammatory Networks during Cellular Senescence: Causes and Consequences." *Trends Mol Med* 16, no. 5 (2010): 238–46.
31. Menendez, J. A., and T. Alarcon. "Senescence-Inflammatory Regulation of Reparative Cellular Reprogramming in Aging and Cancer." *Front Cell Dev Biol* 5 (2017): 49.
32. Pathak, R. U., M. Soujanya, and R. K. Mishra. "Deterioration of Nuclear Morphology and Architecture: A Hallmark of Senescence and Aging." *Ageing Res Rev* 67 (2021): 101264.
33. Heckenbach, I., G. V. Mkrtchyan, M. B. Ezra, D. Bakula, J. S. Madsen, M. H. Nielsen, D. Oro, B. Osborne, A. J. Covarrubias, M. L. Idda, M. Gorospe, L. Mortensen, E. Verdin, R. Westendorp, and M. Scheibye-Knudsen. "Nuclear Morphology Is a Deep Learning Biomarker of Cellular Senescence." *Nat Aging* 2, no. 8 (2022): 742–55.
34. Dimri, G. P., X. Lee, G. Basile, M. Acosta, G. Scott, C. Roskelley, E. E. Medrano, M. Linskens, I. Rubelj, O. Pereira-Smith, and et al. "A Biomarker That Identifies Senescent Human Cells in Culture and in Aging Skin in Vivo." *Proc Natl Acad Sci U S A* 92, no. 20 (1995): 9363–7.
35. Tragoonlugkana, P., C. Pruksapong, P. Ontong, W. Kamprom, and A. Supokawej. "Fibronectin and Vitronectin Alleviate Adipose-Derived Stem Cells Senescence during Long-Term Culture through the Akt/Mdm2/P53 Pathway." *Sci Rep* 14, no. 1 (2024): 14242.
36. Matsuo, M., H. Sakurai, Y. Ueno, O. Ohtani, and I. Saiki. "Activation of Mek/Erk and Pi3k/Akt Pathways by Fibronectin Requires Integrin Alphav-Mediated Adam Activity in Hepatocellular Carcinoma: A Novel Functional Target for Gefitinib." *Cancer Sci* 97, no. 2 (2006): 155–62.
37. Veevers-Lowe, Jennifer, Stephen G. Ball, Adrian Shuttleworth, and Cay M. Kielty. "Mesenchymal Stem Cell Migration Is Regulated by Fibronectin through A5β1-Integrin-Mediated Activation of Pdgfr-B and Potentiation of Growth Factor Signals." *Journal of Cell Science* 124, no. 8 (2011): 1288–300.